An in Situ Study of the Adsorption Behavior of Functionalized Particles on Self-Assembled Monolayers via Different Chemical Interactions

Xing Yi Ling,[§,†] Laurent Malaquin,[||,†,‡] David N. Reinhoudt,[§] Heiko Wolf,*[,||] and Jurriaan Huskens*[,§]

Laboratories of Molecular Nanofabrication and Supramolecular Chemistry and Technology, MESA+ Institute for Nanotechnology, University of Twente, P.O. Box 217, Enschede 7500 AE, The Netherlands, and IBM Research GmbH, Zurich Laboratory, Säumerstrasse 4, CH-8803 Rüschlikon, Switzerland

Received June 6, 2007. In Final Form: July 15, 2007

The formation of particle monolayers by convective assembly was studied in situ with three different kinds of particle−surface interactions: adsorption onto native surfaces, with additional electrostatic interactions, and with supramolecular host−guest interactions. In the first case carboxylate-functionalized polystyrene (PS−COOH) particles were assembled onto native silicon oxide surfaces, in the second PS−COOH onto protonated amino-functionalized (NH_3^+) self-assembled monolayers (SAMs), and in the third β-CD-functionalized polystyrene (PS−CD) particles onto β-CD SAMs with pre-adsorbed ferrocenyl-functionalized dendrimers. The adsorption and desorption behaviors of particles onto and from these surfaces were observed in situ on a horizontal deposition setup, and the packing density and order of the adsorbed particle lattices were compared. The desorption behavior of particles from surfaces was evaluated by reducing the temperature below the dew point, thus initiating water condensation. Particle lattices on native oxide surfaces formed the best hexagonal close packed (hcp) order and could be easily desorbed by reducing the temperature to below the dew point. The electrostatically modified assembly resulted in densely packed, but disordered particle lattices. The specificity and selectivity of the supramolecular assembly process were optimized by the use of ferrocenyl-functionalized dendrimers of low generation and by the introduction of competitive interaction by native β-CD molecules during the assembly. The fine-tuned supramolecularly formed particle lattices were nearly hcp packed. Both electrostatically and supramolecularly formed lattices of particles were strongly attached to the surfaces and could not be removed by condensation.

Introduction

Building up ordered nanostructures from particles has attracted a lot of interest due to the need for miniaturization.[1] The intriguing chemical, electronic, and surface properties that arise from such individual or organized nanometer-sized objects makes them suitable for electronic, optical, and biological applications.[2] In general, there are two approaches to assemble nanostructured materials, namely, physical assembly and supramolecular assembly. The physical assembly technique is based on "let nature do its work",[3] which includes methods such as convective or capillary assembly,[4,5] spin coating,[6] colloidal epitaxy,[7] etc. In particular, convective assembly is a simple technique that has been frequently employed to integrate non-functionalized particles into highly hexagonally ordered and close packed single or multilayered particle lattices.[8]

The mechanism of convective assembly has been extensively studied by Nagayama et al.[9] The major driving force for the assembly is the evaporation of water from the particle suspension. Mobile particles in a thin liquid film are convectively assembled as a result of the hydrodynamic forces induced by the influx of water close to the drying edge. In general, the particles and surfaces are non-functionalized and hydrophilic, which causes a stable thin liquid layer to be formed at the drying edge with a thickness comparable to the particle diameter. The assembly process starts when the thickness of the solvent layer becomes smaller than the particle diameter.[10] The combined effects of the convective flow and the attractive capillary forces arise when the tops of the particles protrude from the solvent layer, leading to the formation of extended layers or multilayers of closely packed particles, by which the local or global free energy reaches a minimum.[11] However, this technique provides limited control over the structure of the particle lattices and the dimensions and complexity of the final assemblies.

Supramolecular assembly utilizes coupling chemistries to precisely direct and control the deposition of functionalized particles onto the substrate, possibly in more complex patterns, where physical assembly of non-functionalized particles is not possible. Typical chemical approaches are electrostatic interactions,[12] host−guest interactions,[13] and thiol-based self-assembly.[14] In supramolecular assembly, the organization of the particle lattice

* Authors to whom correspondence may be sent. E-mail: (H.W.) hwo@zurich.ibm.com; (J.H.) j.huskens@utwente.nl.

§ University of Twente.

|| IBM Research GmbH, Zurich Laboratory.

† These authors contributed equally to this work.

‡ Present address: Laboratoire de Photonique et de Nanostructures, Route de Nozay, 91460 Marcoussis, France.

(1) Arsenault, A.; Fournier-Bidoz, S.; Hatton, B.; Míguez, H.; Tétreault, N.; Vekris, E.; Wong, S.; Yang, S. M.; Kitaev, V.; Ozin, G. A. *J. Mater. Chem.* **2004**, *14*, 781.

(2) Shipway, A. N.; Katz, E.; Willner, I. *ChemPhysChem.* **2000**, *1*, 18.

(3) Wang, D.; Möhwald, H. *J. Mater. Chem.* **2004**, *14*, 459.

(4) Murray, C. B.; Kagan, C. R.; Bawendi, M. G. *Science* **1995**, *270*, 1335.

(5) Gates, B.; Qin, D.; Xia, Y. *Adv. Mater.* **1999**, *11*, 466.

(6) Ozin, G. A.; Yang, S. M. *Adv. Funct. Mater.* **2001**, *11*, 95.

(7) Van Blaaderen, A.; Ruel, R.; Wiltzius, P. *Nature* **1997**, *385*, 321.

(8) Zhang, J.; Alsayed, A.; Lin, K. H.; Sanyal, S.; Zhang, F.; Pao, W.-J.; Balagurusamy, V. S. K.; Heiney, P. A.; Yodha, A. G. *Appl. Phys. Lett.* **2002**, *81*, 3176.

(9) Denkov, N. D.; Velev, O. D.; Kralchevsky, P. A.; Ivanov, I. B.; Yoshimura, H.; Nagayama, K. *Nature* **1993**, *361*, 26.

(10) Paunov, V. N.; Kralchevsky, P. A.; Denkov, N. D.; Nagayama, K. *J. Colloid Interface Sci.* **1993**, *157*, 100.

(11) Nagayama, K. *Colloids Surf., A.* **1996**, *109*, 363.

(12) Decher, G.; Hong, J. D.; Schmitt, J. *Thin Solid Films* **1992**, *210* and *211*, 831.

10.1021/la701671s CCC: $37.00
Published on Web 08/18/2007

will no longer depend solely on surface tension and long-range attractive forces that act in a lateral direction, but rather on the competition between *lateral* attractive forces and *vertical* supramolecular interactions between functionalized particles and the surface. Electrostatics, owing to its simplicity, has been widely used to assemble chemically functionalized particles onto a surface via the attractive force between two oppositely charged surfaces. Jonas et al., Hammond et al., and our group have independently reported the selective adsorption (by drop casting) of negatively charged particles onto chemically patterned surfaces.[15−17] The parameters of the adsorption of particles into patterns, e.g., pH, drying conditions, ionic strength, and surfactant concentration, were extensively studied. In all cases, the ordering of the particle lattice was imperfect owing to strong binding affinity of the particles for the surface.

Supramolecular host−guest interactions have been exploited for the assembly of receptor-functionalized molecules or particles onto interfaces with molecular recognition abilities. Similar to biomolecules in nature, the "host" molecules are to interact specifically with complementary "guest" molecules to form noncovalent host−guest pairs, for instance crown ether complexation by ammonium SAMs,[18] His-tagged proteins by a Ni-nitrilotriacetic acid-presenting surface,[19] etc. Multivalency is used to enhance the binding affinities and specificities between host and guest as these noncovalent interactions are kinetically labile and are continuously broken and formed.[20,21] Recently, our group introduced the concept of "molecular printboards", i.e. β-cyclodextrin (β-CD) SAMs on gold or silicon oxide substrates that possess supramolecular host properties.[22,23] On these β-CD SAMs, complementary multivalent guest-functionalized dendrimer molecules were adsorbed, resulting in the formation of kinetically stable supramolecular assemblies.[24−26] With the aid of adamantyl- or ferrocenyl-functionalized dendrimers as a noncovalent supramolecular glue, β-CD-functionalized gold and silica nanoparticles were assembled onto β-CD SAMs.[13,27,28] Apart from the formation of multivalent and stable assemblies, the supramolecular interaction is also appealing for its highly tunable binding strength. Different guest molecules (e.g., ferrocenyl, adamantyl, etc.) with different binding strengths can be selected to bind to the β-CD SAMs with different binding strengths.[29] The total number of interactions involved in the assembly can be easily varied by using dendrimers of different generations, therefore altering the total binding strength during the assembly. Competition can be introduced when native β-CD molecules are added to the particle suspension so that β-CD hosts on particle surfaces have to compete with the native β-CD to couple to the surface of the pre-adsorbed guest-functionalized dendrimers on the β-CD SAM.

Here we describe an in situ study of the adsorption and desorption behavior of particles onto and from surfaces for three different kinds of particle−surface interactions, i.e., convective assembly on surfaces, with additional electrostatic interactions and with supramolecular host−guest interactions. The aim was to compare the packing order and density of the particle lattices as a result of different binding affinities between the particles and the surfaces. For the ease of visualization, poly(styrene-*co*-acrylic acid) particles with or without β-CD functionality of about 450 nm in diameter were synthesized and employed in all experiments. The desorption behavior of the particles from the surfaces was evaluated by reducing the temperature to below the condensation temperature.[30] In particular, the supramolecular particle assembly was further fine-tuned by using ferrocenyl dendrimers of different generations and by introducing competition by adding native β-CD molecules into the particle suspension. Furthermore, the influences of these different assembly schemes on the creation of particle stripes on patterned substrates were studied.

Experimental Details

Chemicals. Styrene, divinylbenzene, acrylic acid, *N*-(3-dimethylaminopropyl)-*N*-ethylcarbodiimide hydrochloride (EDC), *N*-hydroxysuccinimide (NHS), 3-aminopropyl triethoxysilane (APTES), *N*-[3-(trimethoxysilyl)propyl]ethylenediamine, and 1,4-phenylene diisothiocyanate were obtained from commercial sources (Sigma Aldrich, Germany). Buffer solutions of all pHs were prepared as described previously, unless otherwise stated.[27] β-Cyclodextrin (β-CD) heptamine, adamantyl-terminated poly(propylene imine) dendrimer of generation 5 (G5-PPI-$(Ad)_{64}$), ferrocenyl-functionalized poly(propylene imine) dendrimer of generations 1 and 3 (G1-PPI-$(Fc)_4$ and G3-PPI-$(Fc)_{16}$) were synthesized as described before.[28,31,32] Milli-Q water with a resistivity higher than 18 MΩ·cm was used in all experiments.

Preparation of Carboxylate-Functionalized Polystyrene Particles (3, PS−COOH). The core−shell particles of poly(styrene-*co*-acrylic acid) (PS−COOH) were prepared as described before.[33,34] Milli-Q water (100 mL) was stirred and heated to 80 °C under N_2 atmosphere. Eleven milliliters of styrene and 1 mL of divinylbenzene were then added quickly into the solution. The mixture was stirred for another 20 min before adding 5 mL of 0.1 M aqueous potassium persulfate. The mixture was stirred for another 4 h under N_2 atmosphere. One milliliter of distilled acrylic acid and 2.6 mL of 0.1 M potassium persulfate were added, and the reaction was continued for another 75 min. The reaction product was centrifuged and redispersed in water (pH 7.0) for at least three times.

Preparation of β-Cyclodextrin-Functionalized Polystyrene Particles (5, PS−CD). The attachment of β-cyclodextrin onto the surface of PS−COOH particles was based on a functionalization

(13) Crespo-Biel, O.; Dordi, B.; Reinhoudt, D. N.; Huskens, J. *J. Am. Chem. Soc.* **2005**, *127*, 7594.
(14) Kiely, C. J.; Fink, J.; Brust, M.; Bethell, D.; Schiffrin, D. J. *Nature* **1998**, *396*, 444.
(15) Jonas, U.; del Campo, A.; Kruger, C.; Glasser, G.; Boos, D. *Proc. Natl. Acad. Sci. U.S.A.* **2002**, *99*, 5034.
(16) Chen, K. M.; Jiang, X.; Kimerling, L. C.; Hammond, P. T. *Langmuir* **2000**, *16*, 7825.
(17) Maury, P.; Escalante, M.; Reinhoudt, D. N.; Huskens, J. *Adv. Mater.* **2005**, *17*, 2718.
(18) Arias, F.; Godinez, L. A.; Wilson, S. R.; Kaifer, A. E.; Echegoyen, L. *J. Am. Chem. Soc.* **1996**, *118*, 6086.
(19) Dietrich, C.; Schmitt, L.; Tample, R. *Proc. Natl. Acad. Sci. U.S.A.* **1995**, *92*, 9014.
(20) Mulder, A.; Huskens, J.; Reinhoudt, D. N. *Org. Biomol. Chem.* **2004**, *2*, 3409.
(21) Reinhoudt, D. N.; Crego-Calama, M. *Science* **2002**, *295*, 2403.
(22) Beulen, M. W. J.; Bügler, J.; Lammerink, B.; Geurts, F. A. J.; Biemond, E. M. E. F.; Van Leerdam, K. G. C.; Van Veggel, F. C. J. M.; Engbersen, J. F. J.; Reinhoudt, D. N. *Langmuir* **1998**, *14*, 6424.
(23) Onclin, S.; Mulder, A.; Huskens, J.; Ravoo, B. J.; Reinhoudt, D. N. *Langmuir* **2004**, *20*, 5460.
(24) Huskens, J.; Deij, M. A.; Reinhoudt, D. N. *Angew. Chem., Int. Ed.* **2002**, *41*, 4467.
(25) Auletta, T.; Dordi, B.; Mulder, A.; Sartori, A.; Onclin, S.; Bruinink, C. M.; Péter, M.; Nijhuis, C. A.; Beijleveld, H.; Schönherr, H.; Vancso, G. J.; Casnati, A.; Ungaro, R.; Ravoo, B. J.; Huskens, J.; Reinhoudt, D. N. *Angew. Chem., Int. Ed.* **2004**, *43*, 369.
(26) Nijhuis, C. A.; Huskens, J.; Reinhoudt, D. N. *J. Am. Chem. Soc.* **2004**, *126*, 12266.
(27) Mahalingam, V.; Onclin, S.; Péter, M.; Ravoo, B. J.; Huskens, J.; Reinhoudt, D. N. *Langmuir* **2004**, *20*, 11756.
(28) Nijhuis, C. A.; Huskens, J.; Reinhoudt, D. N. *J. Am. Chem. Soc.* **2004**, *126*, 12266.
(29) Rekharsky, M. V.; Inoue, Y. *Chem. Rev.* **1998**, *98*, 1875.
(30) Malaquin, L.; Kraus, T.; Schmid, H.; Delamarche, E.; Wolf, H. *Langmuir*, accepted.
(31) Michels, J. J.; Baars, M. W. P. L.; Meijer, E. W.; Huskens, J.; Reinhoudt, D. N. *J. Chem. Soc., Perkin Trans. 2* **2000**, 1914.
(32) Guillo, F.; Jullien, L.; Hamelin, B.; Lehn, J.-M.; De Robertis, L.; Driguez, H. *Bull. Soc. Chim. Fr.* **1995**, *132*, 857.
(33) Greci, M. T.; Pathak, S.; Mercado, K.; Prakash, G. K. S.; Thompson, M. E.; Olah, G. A. *J. Nanosci. Nanotechnol.* **2001**, *1*, 3.
(34) Wang, Y.; Wang, Y.; Feng, L. *J. Appl. Polym. Sci.* **1997**, *64*, 1843.

Scheme 1. Preparation of Carboxylate- and β-Cyclodextrin-Functionalized Poly(styrene-*co*-acrylic acid) Particles

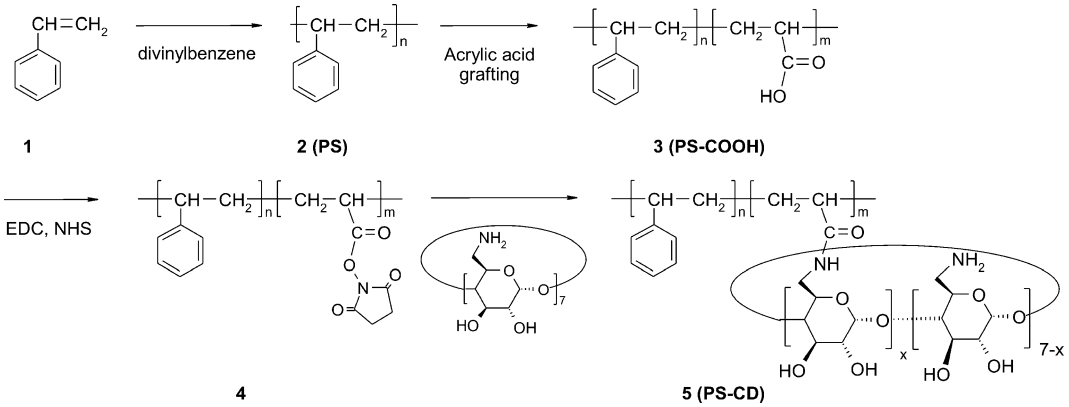

strategy for β-cyclodextrin-functionalized silica particles.[27] PS−COOH (24 mL, 11 wt %) was redispersed in MES buffer (pH 5.6) and was added to 10 mL of 5 mM EDC/NHS mixture. After 1 h stirring, the particles **3** were centrifuged and redispersed in a carbonate buffer (pH 9.6). This suspension was added dropwise to 5 mL of 5 mM aqueous β-CD heptamine. Stirring was continued overnight at room temperature. The final product, β-CD-functionalized poly(styrene-*co*-acrylic acid) (**4**, PS−CD) particles were centrifuged and redispersed in 10 mM carbonate buffer (pH 9.6) for at least three times to remove unreacted β-CD heptamine from the mixture.

Substrate and Monolayer Preparation. Cleaned silicon substrates were prepared by immersion in piranha solution (conc H_2SO_4 and 33% H_2O_2 in a 3:1 volume ratio [**Warning!** Piranha should be handled with caution; it can detonate unexpectedly.]) for 15 min to form a SiO_2 layer on the surface. The substrates were then sonicated in Milli-Q water and ethanol for 1 min and dried with N_2. Amino-terminated SAMs were obtained by gas-phase evaporation of APTES in a desiccator under vacuum. The samples were left several hours and then carefully rinsed with ethanol and Milli-Q water. β-CD SAMs were obtained according to a published procedure.[23,35] In brief, the substrates were functionalized *N*-[3-(trimethoxysilyl)propyl]-ethylenediamine by gas-phase evaporation. Transformation of the amino-terminated SAMs to isothiocyanate-bearing layers was accomplished by exposure to an ethanol solution of 1,4-phenylene diisothiocyanate at 50 °C for 2 h. β-CD SAMs were finally obtained by reaction of the isothiocyanate-terminated monolayer with β-CD heptamine in pH 7.5 water, at 50 °C for 2 h. The adsorption of G1-PPI-$(Fc)_4$ or G3-PPI-$(Fc)_{16}$ was achieved by immersing the β-CD SAM substrates in a aqueous solution of G1-PPI-$(Fc)_4$ and/or G3-PPI-$(Fc)_{16}$ (1 mM Fc functionality) for 30 min, followed by rinsing with 10 mM aqueous β-CD at pH 2 and Milli-Q water.

Particle Assembly. A defined volume (40 μL) of 0.2 wt % of particle suspension in was injected between the SAM and a glass slide (Figure 2). The liquid meniscus was moved over the SAM at a constant velocity of 1 μm/s. The entire setup was installed on the stage of an optical microscope for direct observation and control of the assembly process. A Peltier element allowed the temperature of the template to be controlled.[30] Typically, the adsorption of particles was performed at a temperature of about 18 °C, whereas the desorption was attempted at a temperature below 6 °C.

Nanoimprint Lithography (NIL). Silicon stamps were made by photolithography followed by reactive ion etching (RIE, Elektrotech Twin system PF 340). A stamp consisted of 3.5 μm lines at 7.5 μm period with a height of 500 nm. A piranha-cleaned silicon substrate was first spin-coated with a 500-nm thick layer of PMMA. Stamp and substrate were put in contact, and a pressure of 40 bar was applied at a temperature of 180 °C using a hydraulic press (Specac). The residual layer was removed by dipping the samples in acetone during 30 s.

Fourier Transform Infrared (FT-IR) Spectroscopy. Infrared spectra were recorded on a Perkin-Elmer Spectrum BX spectrometer, using KBr pellets that contained 2−5 mg of particles.

Dynamic Light Scattering (DLS). DLS experiments were performed with a Zetasizer 4000 (Malvern Instruments Ltd., U.K.) at 25 °C using a laser wavelength of 633 nm at a scattering angle of 90°. Results obtained are the averages of three measurements. The average hydrodynamic diameter (d_{av}) of the particles was determined on 1.5-mL samples in corresponding solutions. The dispersions were gently shaken before the measurements for proper mixing. The (attempted) aggregation of PS−COOH and PS−CD with the adamantyl-terminated PPI dendrimer, generation 5 (Ad-PPI-G5), was performed by measuring d_{av} for a 1-mL sample before and after subsequent additions of 40, 130, 250, and 500 μL of a 0.2 mM solution of Ad-PPI-G5.[24,27] The dispersions were gently shaken before the measurements for proper mixing.

Zeta Potential. Zeta potentials of the silica particles were obtained with a Zetasizer 2000 (Malvern Instruments Ltd., U.K.) using the laser doppler velocimetry technique. In this technique, the velocity of suspended particles is measured as function of an applied electrical field, which correlates with the particle motion. Measurements were performed at 25 °C using a 1000 Hz modulator frequency and a cell drive voltage of 120 V. The values reported are the averages of 10 measurements.

Contact Angle Goniometry. Contact angles were measured on a Krüss G10 contact angle measuring instrument, equipped with a CCD camera. Advancing contact angles were determined automatically during growth of the droplet of Milli-Q water by a drop-shape analysis routine.

Scanning Electron Microscopy (SEM). All SEM images were taken with a HR-LEO 1550 FEF SEM.

Results and Discussion

Preparation and Characterization of PS−COOH and PS−CD Particles. Core−shell particles of poly(styrene-*co*-acrylic acid) (PS−COOH) were prepared by seeded emulsifier-free emulsion polymerization.[33,34] Polystyrene core particles (**2**, PS) were prepared first using divinylbenzene as a cross-linker. When the conversion of styrene to polystyrene was nearly complete, acrylic acid was grafted subsequently onto the surface of polystyrene, forming poly(styrene-*co*-acrylic acid) (**3**, PS−COOH) core−shell particles. The carboxylic acid groups of PS−COOH were then converted to activated ester groups by using EDC/NHS to form **4**. The attachment of β-CD was performed by reacting **4** with β-CD heptamine, forming **5** (PS−CD)[27] (Scheme 1).

The conversion of styrene and acrylic acid to polystyrene and subsequently to poly(styrene-*co*-acrylic acid) was followed by gravimetry, which showed ∼98% and 100% conversion, respectively.[36] Samples of PS and PS−COOH particles were collected before and after the grafting of acrylic acid, respectively,

(35) Ling, X. Y.; Reinhoudt, D. N.; Huskens, J. *Langmuir* **2006**, *22*, 8777.

(36) Shim, S.-E.; Cha, Y.-J.; Byun, J.-M.; Choe, S. *J. Appl. Polym. Sci.* **1999**, *71*, 2259.

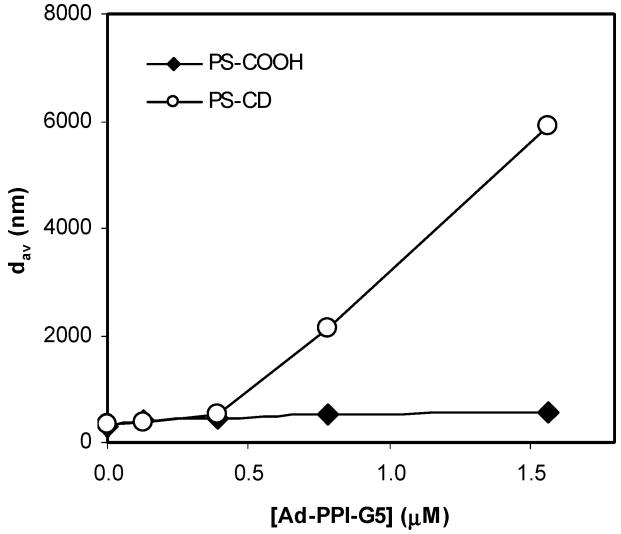

Figure 1. The average hydrodynamic diameter (d_{av}) of PS−COOH (◆) and PS−CD (○) particles as a function of the concentration of G5-PPI-$(Ad)_{64}$.

and made into KBr pellets for FTIR measurements. The spectrum of PS−COOH was similar to that of PS, with aromatic CH stretching bands at 1493 and 3010 cm^{-1}; aromatic C═C stretch at 1599 cm^{-1}, and C−C vibrational bands observed at 700, 760, 1030, 1080 cm^{-1} (Supporting Information, Figure S1).[34,37] CH_2 stretching was also seen at 2920 cm^{-1} for both samples. A distinctive peak at 1710 cm^{-1} was only observed for PS−COOH, which clearly indicated the presence of C═O groups.

As PS−COOH and PS−CD were prepared from the same batch of reaction, their size and size distribution were not expected to differ. The average particle diameter distribution of PS−COOH was 450 ± 30 nm, as determined by SEM (Supporting Information, Figure S2).

The host−guest complexation ability of PS−CD in solution in the presence of multivalent guest molecules was determined by DLS. The concept is that a known amount of multivalent guest molecules is added to the measuring particle suspension (concentration of $\sim 4 \times 10^{11}$ particles/mL)[38] such that the multiple binding sites on a guest molecule simultaneously bind two or more adjacent particles. As a result, aggregation occurs which leads to an increase of the hydrodynamic diameter. We used the adamantyl-terminated poly(propylene imine) dendrimer of generation 5 (G5-PPI-$(Ad)_{64}$), which has 64 adamantyl groups for the complexation with β-CD in solution.[31] The change in average hydrodynamic diameter of particle dispersions of PS−COOH and PS−CD in carbonate buffer as a function of the concentration of G5-PPI-$(Ad)_{64}$ is shown in Figure 1. When the amount of multivalent guest molecules was slowly increased, a drastic increase in hydrodynamic diameter of the PS−CD particle suspension was observed, indicative of supramolecular aggregation. In contrast, only a small increase in hydrodynamic radius for PS−COOH was observed, possibly due to electrostatic interactions between the positively charged dendrimers and negatively charged particles in carbonate buffer. This experiment indirectly confirms the presence of β-cyclodextrin on the surface of PS−CD.

The concentration of β-CD in the PS−CD particle suspension can be estimated from this aggregation experiment.[27] From Figure 1, the aggregation starts when [G5-PPI-$(Ad)_{64}$] > 0.5 μM, which is equivalent to an adamantyl concentration of 32 μM. The aggregation becomes more distinguished with an increase in G5-PPI-$(Ad)_{64}$ concentration. Assuming the aggregation sets off when the [Ad]/[β-CD] molar ratio is greater than 1,[39] the concentration of β-CD in the PS−CD particle suspension can be estimated to be ∼32 μM, i.e., 48,000 β-CD molecules occupying on surface of each particle. These observations suggest that the concentration of β-CD on the PS−CD particles is lower than the β-CD heptathioether formed on a gold substrate,[26] but still sufficiently high for effective multivalent host−guest interactions.

The surface charges of PS−COOH and PS−CD were examined by using zeta potential measurements (Supporting Information, Figure S3). Buffers from pH 4.0 to 9.0 were used in this study. Both PS−COOH and PS−CD exhibited nearly similar negative charges at all pHs. For pH 5−9, ζ values between −40 and −50 mV were recorded. Only when lowering the pH to 4, a ζ of about −25 mV was observed, which is attributed to partial protonation of the acrylic acid groups ($pK_a \approx 4.5$). The similarity between PS−COOH and PS−CD is justified by the core−shell nature of the poly(styrene-*co*-acrylic acid) particles, and by noting that an excess of unreacted carboxylic acid groups remains on the surface of PS−CD, because only the outer groups react with β-CD heptamine.

Assembly of Particles on Nonpatterned Flat Surfaces. The adsorption and desorption behavior of the functionalized particles on various substrates was observed in situ by optical microscopy. We focused our studies on three basic assembly schemes, i.e., convective assembly onto native oxide substrates, assembly with additional electrostatic interactions, and assembly with supramolecular (host−guest) interactions. As shown in Scheme 2, these interaction systems are represented by adsorption of carboxylate-functionalized polystyrene (PS−COOH) particles onto the native SiO_2 surfaces of piranha-cleaned silicon, PS−COOH onto protonated amino-functionalized (NH_3^+) SAMs, and β-CD-functionalized polystyrene (PS−CD) particles onto β-CD SAMs with pre-adsorbed ferrocenyl-functionalized dendrimers as a supramolecular glue (Scheme 3).

The polarity of the surface groups of self-assembled monolayers (SAMs) was examined by contact angle goniometry. The contact angle of each monolayer plays a crucial role in the adsorption of particles at the liquid−air−solid boundary. Table 1 summarizes the advancing contact angles (θ_a) of water on different SAMs. The native SiO_2 substrate exhibited a high wettability with an advancing angle of less than 20°, due to the presence of silanol groups on the surface. The APTES (NH_2) monolayer has an advancing angle of 60°. The advancing angle was reduced to 30° upon protonation of the NH_2 groups to NH_3^+ by dipping the SAM in a 0.1 M aqueous HCl for 1 min. The β-CD monolayer on silicon was prepared as described before, with a θ_a of 50°.[23] Complementary guest molecules, G1-PPI-$(Fc)_4$ and G3-PPI-$(Fc)_{16}$ were adsorbed onto the β-CD SAM by immersing the β-CD SAMs in the respective dendrimer solutions for 30 min, followed by rinsing with 10 mM β-CD solution and water to remove any physisorbed material. Due to the hydrophobic nature of the ferrocenyl moieties, the θ_a increased to 60° and 63°, for G1-PPI-$(Fc)_4$ and G3-PPI-$(Fc)_{16}$, respectively.

In order to quantify the amount of ferrocenyl dendrimers on the β-CD SAM, G1-PPI-$(Fc)_4$ and G3-PPI-$(Fc)_{16}$ were adsorbed onto β-CD SAMs on gold, and the cyclic voltammograms (CV) of both substrates were recorded (Supporting Information, Figure S4). By integrating the areas under the peaks, the total charges

(37) Bhutto, A. A.; Vesely, D.; Gabrys, B. J. *Polymer* **2003**, *44*, 6627.
(38) Based on 2 wt % solution of particles, with a polystyrene density of 1.05 kg/dm^3.
(39) Crespo-Biel, O.; Juković, A.; Karlsson, M.; Reinhoudt, D. N.; Huskens, J. *Isr. J. Chem.* **2005**, *45*, 353.

Scheme 2. Schematic Illustrations (not to scale) of Three Particle Assembly Schemes, i.e., Convective Assembly of PS−COOH on the Native SiO_2 Surface of Silicon (A), Convective Assembly with Additional Electrostatic Interactions of PS−COOH with an NH_3^+ SAM (B), and Convective Assembly with Supramolecular Interactions of PS−CD with Complementary Pre-adsorbed Ferrocenyl-Functionalized Dendrimers on a β-CD SAM

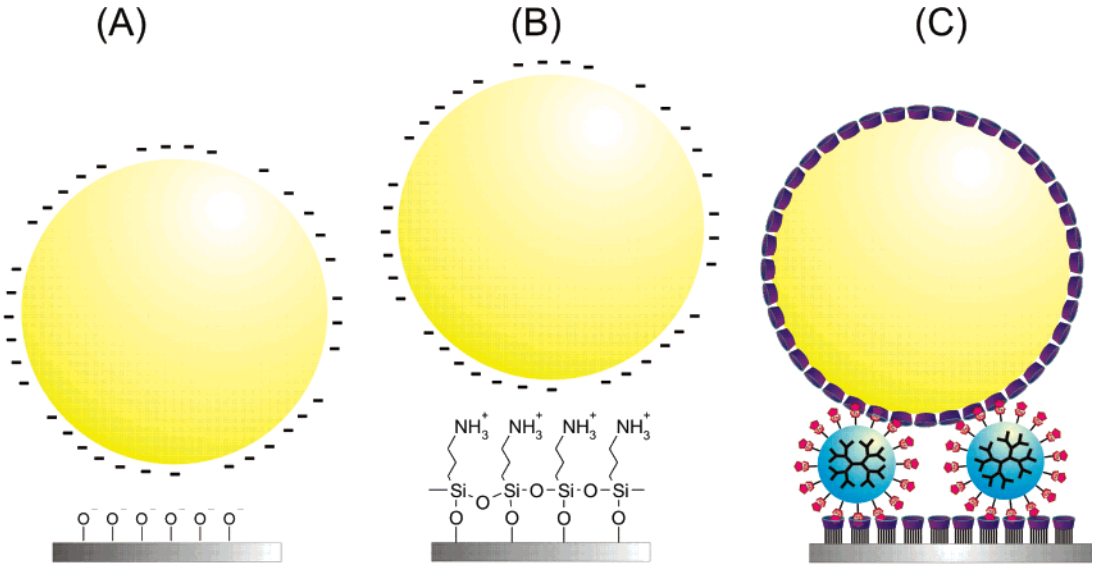

of the first oxidation cycle were obtained. The total charges can be converted to surface coverage of ferrocene moieties (Fc), which were 8.7×10^{-11} and 3.7×10^{-10} mol/cm^2 for G1-PPI-$(Fc)_4$ and G3-PPI-$(Fc)_{16}$, respectively.[28] Considering the numbers of Fc endgroups and binding stoichiometries of G1-PPI-$(Fc)_4$ and G3-PPI-$(Fc)_{16}$, 50% and 100% of the β-CDs on the SAMs were coupled with G1-PPI-$(Fc)_4$ and G3-PPI-$(Fc)_{16}$, respectively.[40] The lower coverage of G1-PPI-$(Fc)_4$ is attributed to partial desorption of G1-PPI-$(Fc)_4$ from the host surface by competitive interaction with native β-CD solution during the rinsing procedure, in line with the relatively weak interaction of this dendrimer.[41] It should be noted that not all available ferrocene moieties on a dendrimer will bind to the β-CD host surface. Only 2 Fc endgroups of G1-PPI-$(Fc)_4$ (total 4 Fc moieties) and 4 Fc endgroups of G3-PPI-$(Fc)_{16}$ (total 16 Fc moieties) will couple to the β-CD SAM at each time.[28] For these ferrocenyl dendrimers sized between 2 and 4 nm, the surface of a PS−CD particle of 450 nm can be considered as a flat β-CD SAM. Hence, the numbers of interactions for a single G1-PPI-$(Fc)_4$ and G3-PPI-$(Fc)_{16}$ dendrimer with a particle is expected to be 2 and 4 per dendrimer, respectively.

The adsorption and desorption behavior of the functionalized particles on various substrates were observed in situ under the optical microscope with convective assembly as a driving assembly scheme. Figure 2 illustrates the experimental setup used for the particle assembly. A droplet of 0.2 wt % of particle suspension was added into the gap between a mobile substrate and a fixed glass slide while the temperature was controlled between 4 and 20 °C. The substrate was then shifted to the left at a constant velocity (0.1−1 μm/s). For ease of discussion, the substrate was categorized into two sections, i.e., the assembly and bulk suspension zones. Particles assemble on the surface in the assembly zone as a result of the convective flow of particles induced by the evaporation solvent at the assembly zone. In the suspension zone, the particle suspension is like that in bulk. Depending on the particle−substrate interaction, adsorption from the suspension onto the substrate may also occur in the suspension zone when specific interactions occur.

Figure 3 shows the SEM micrographs of particle lattices obtained by convective assembly and electrostatic assembly. For the pure convective assembly, the particle solution was adjusted to pH 7 to eliminate any attractive electrostatic interactions between the PS−COOH particles and the SiO_2 substrates ($pK_a = 4-5$). Probably, the interactions are actually repulsive in this case. The convective assembly of PS−COOH particles (Figure 3A) started when the SiO_2 substrate was wetted by the particle suspension, forming a very thin meniscus in the front of the assembly zone. A single layer of highly ordered particles with hexagonal close packing (hcp) was formed. No particles were found on the surface of suspension zone. After the assembly, the temperature of the substrate was gradually reduced from 18 °C to below the dew point (about 6 °C). When condensation of water occurred, the particle lattice started to disintegrate and the particles regained their mobility; finally the particle flux was reversed, and all particles returned to the suspension zone. An analogous observation was made for the assembly of PS−CD particles onto SiO_2 (Figure 3B).

In the case of the electrostatic interactions, the pH of the PS−COOH particle suspension was adjusted to 7.0. At this pH, the acrylic acid groups on the surface of PS−COOH are deprotonated ($pK_a \approx 4.5$) while the NH_2 SAM is protonated ($pK_a \approx 9.0$), which should give rise to a strong electrostatic interaction.[15] A densely occupied and disordered multilayered PS−COOH particle lattice was formed on the NH_3^+ SAM (Figure 3C). As observed in situ, particles adsorbed on the surface in the suspension zone as soon as they contacted the substrate, and they remained immobile on the surface. When decreasing the substrate temperature to below the dew point, the particles with no direct contact with the surface desorbed from the surface. A single layer of particles remained at the surface because of strong electrostatic interactions. These observations contrast with those of the assembly of PS−COOH on native SiO_2 substrates, where the particles are mobile enough to be reorganized to achieve the dense hcp packings and no adsorption occurred in the suspension zone.

(40) The coverage of a β-CD SAM is 8×10^{-11} mol/cm^2. For details, see: Beulen, M. J. W.; Bügler, J.; De Jong, M. R.; Lammerink, B.; Huskens, J.; Schönherr, H.; Vancso, G. J.; Boukamp, B. A.; Wieder, H.; Offenhauser, Knoll, W.; Van Veggel, F. C. J. M.; Reinhoudt, D. N. *Chem. Eur. J.* **2000**, *6*, 1176.

(41) Nijhuis, C. A.; Yu, F.; Knoll, W.; Huskens, J.; Reinhoudt, D. N. *Langmuir* **2005**, *21*, 7866.

Scheme 3. Chemical Structures (from top to bottom) of a β-CD SAM on Silicon and Ferrocenyl-Functionalized Poly(propylene imine) Dendrimers of Generations 1 and 3

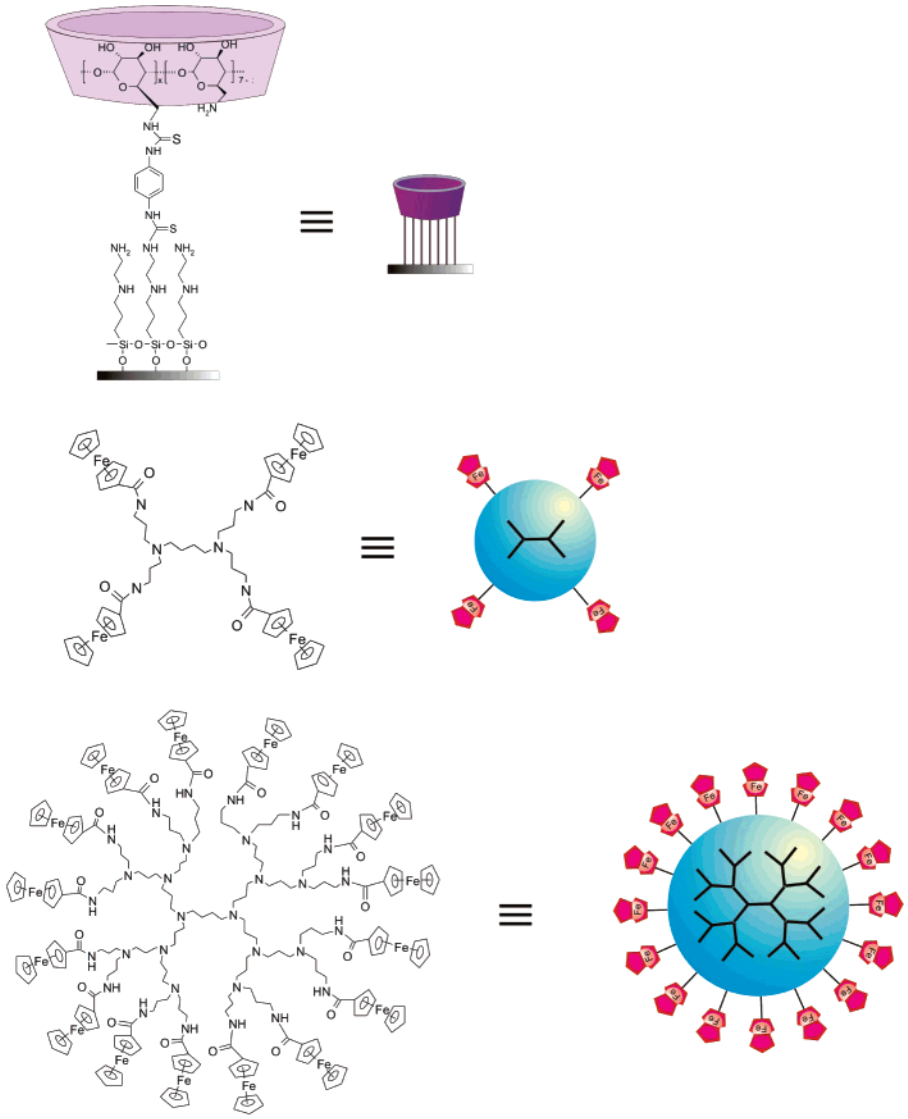

Table 1. Advancing Water Contact Angles (θ_a) on Various Substrates

substrate	θ_a (deg)
native SiO_2 on Si	<20
NH_2 SAM	60
NH_3^+ SAM	30
β-CD SAM	50
G1-PPI-$(Fc)_4$ on β-CD SAM	60
G3-PPI-$(Fc)_{16}$ on β-CD SAM	63

The assembly of PS−CD particles onto a β-CD SAM in the absence of a "supramolecular glue" (ferrocenyl-functionalized dendrimer) was examined. PS−CD particles were dispersed in carbonate buffer in the absence or presence of 5 mM β-CD. The assembly was initiated by wetting the particle suspension on the moderately hydrophilic β-CD SAM surface. The particle lattice formed in the absence of β-CD showed a disordered packing similar to that observed for PS−COOH on an NH_3^+ SAM (not shown). In the presence of β-CD, the particle lattice appeared to have a higher degree of order, although it was not in perfect hcp organization (Figure 3D). The adsorption of particles in the suspension zone was also observed in both cases, once the particle suspension was added, but less so in the case of added β-CD.

It is speculated that the assembly of PS−CD on a β-CD SAM was caused merely by electrostatic interaction. This is because PS−CD particles are negatively charged and a β-CD SAM on silicon is slightly positively charged, as not all NH_2 groups of the SAM react with diisothiocyanate and β-CD heptamine.[23] The tendency to form multilayered particle lattices was most likely attributed to the substrate's low withdrawing velocity, but in part also due to electrostatics.[16] During the desorption by condensation, the particles that had no physical contact with the surface desorbed, possibly because the attractive forces exerted on these particles are weaker.

In order to quantify the degree of ordering of the particle lattice, Voronoi diagrams were created to determine the densities of the particle lattices and the number of non-hexagonally packed particles (defects) over 80−100 μm^2 of a single-layer particle lattice (see Table 2).[42,43] A simple sphere-finding algorithm was used to identify the sphere centers, enabling the construction of a Voronoi diagram which was superimposed on the original image. A particle in a perfect hexagonally packed lattice is surrounded by six neighbors, and they appear as hexagons,

(42) Allen, S. M.; Thomas, E. L. *The Structure of Materials*; Wiley: New York, 1999.
(43) Roerdink, M.; Hempenius, M. A.; Vancso, G. J. *Chem. Mater.* **2005**, *17*, 1275.

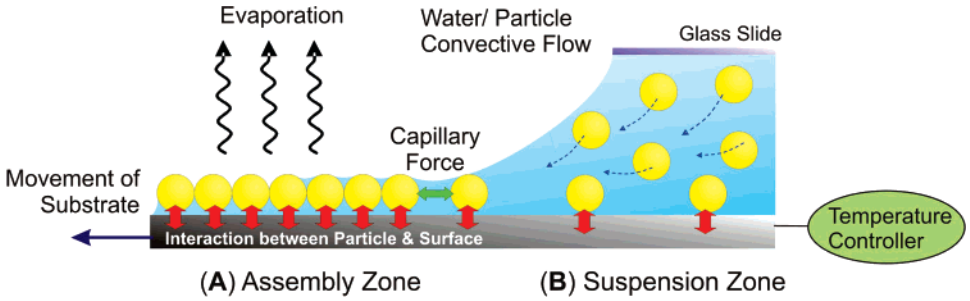

Figure 2. Schematic illustration of the adsorption and assembly of particles on a substrate. On the left, the assembly zone (A) refers to the area where assembly of the particles occurs. The particle assembly is caused by the evaporation of the water meniscus in this area. Between the glass slide and the substrate is the suspension zone (B). Convective flow delivers the particles from the bulk suspension zone to the assembly zone. Additional vertical interactions between the functionalized particles and the substrate may result in adsorption of particles in the suspension zone.

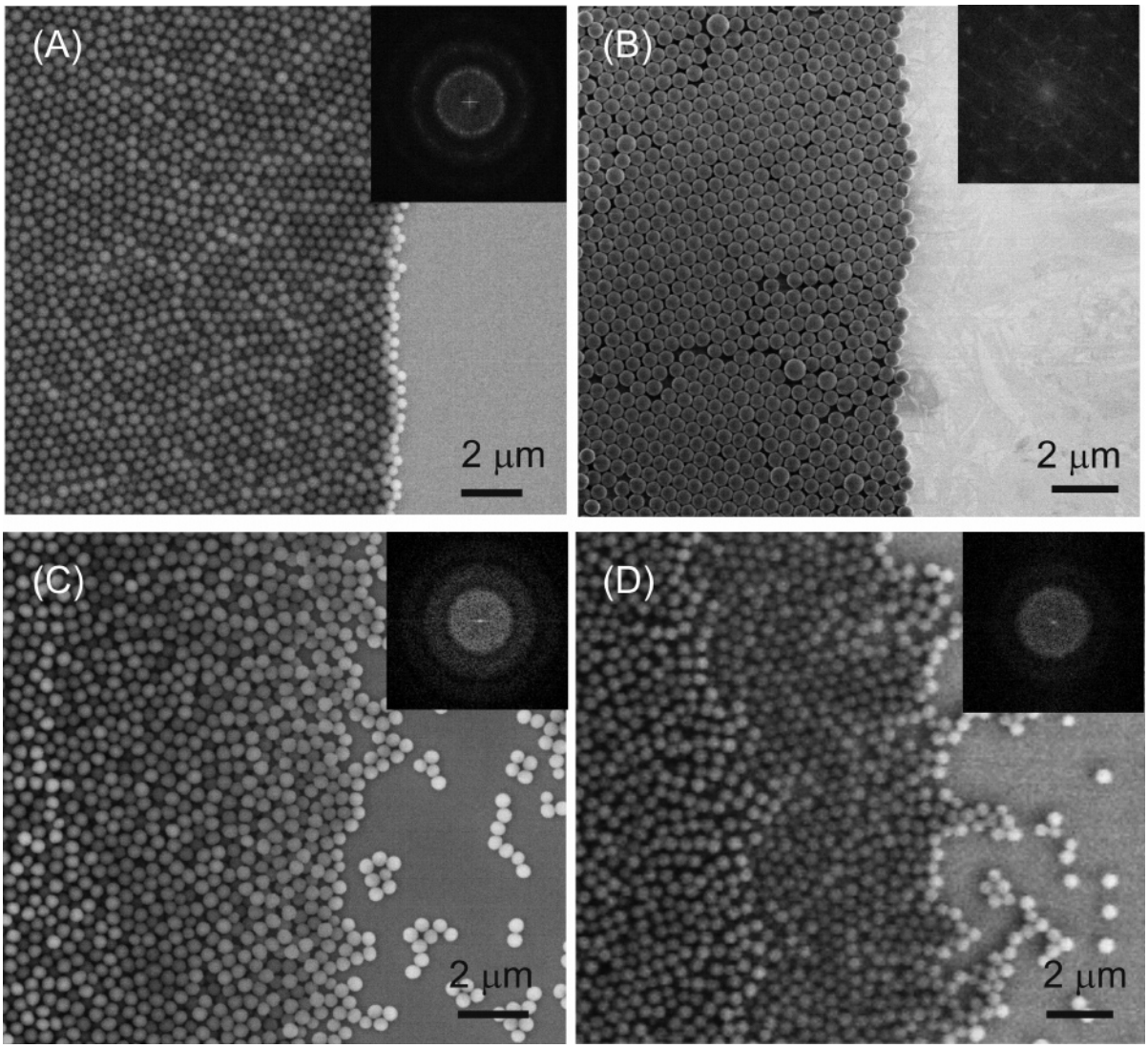

Figure 3. SEM micrographs of the assembled particles formed by adsorption of PS−COOH on native SiO_2 on Si (A), PS−CD on native SiO_2 on Si (B), PS−COOH on NH_3^+ SAM (C), and PS−CD on β-CD SAM (D). The inset at the upper right of each picture shows the 2D Fourier transforms of the respective images.

whereas the non-hexagonally packed particles consist of five- and seven-fold-coordinated sites (see Supporting Information, Figure S5).

The particle densities in the assembly zones of PS−COOH on SiO_2 and PS−CD on SiO_2 are between 5.1 and 5.5 particles/μm^2, which fall in the range of perfect hcp packing order.[44] In contrast, the densities of the electrostatically assembled particle lattices (PS−COOH on NH_3^+ SAM and PS−CD on β-CD SAM) are 3.9−4.8 particle/μm^2, indicating the formation of disordered particle lattices. Approximately 0.7 and 0.8 defects/μm^2 were found for PS−COOH and PS−CD lattices formed on SiO_2, respectively (see Table 2), possibly due to the relatively wide size distribution of particles. The defects of the electrostatically

(44) A perfectly hexagonal close packed particle lattice has a density of 5.4 particles/μm^2, considering the particle size of 450 nm.

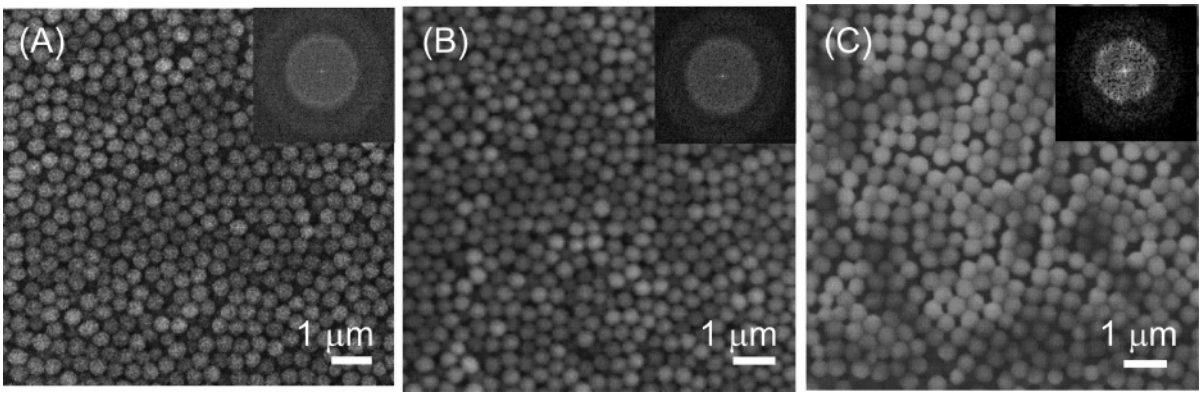

Figure 4. SEM micrographs of particle lattices formed by PS−CD on G3-PPI-$(Fc)_{16}$ pre-adsorbed on a β-CD SAM (A), and PS−CD on G1-PPI-$(Fc)_4$ pre-adsorbed on a β-CD SAM in the absence (B) and presence of 5 mM native β-CD (C). The inset at the upper right of each picture shows the 2D Fourier transforms of the respective images.

Table 2. Comparison of the Densities of Particles Adsorbed onto the Substrate in the Suspension Zone and Assembly Zone, and the Number of Defects (Non-hexagonally Packed Particles) per μm^2

assembly type	sample	density in assembly zone (particles/ μm^2)	defects in assembly zone (defects/μm^2)	density in suspension zone (particles/ μm^2)
convective	PS−COOH on SiO_2	5.1	0.7	0.0
	PS−CD on SiO_2	5.5	0.8	0.0
convective and electrostatic	PS−COOH on NH_3^+ SAM	4.8	2.0	0.5
	PS−CD on β-CD SAM	3.9	1.8	0.8
	PS−CD on β-CD SAM[a]	4.3	1.5	0.2
convective and supramolecular	PS−CD on G1-PPI-$(Fc)_4$ on β-CD SAM	4.8	1.4	0.4
	PS−CD on G3-PPI-$(Fc)_{16}$ on β-CD SAM	4.8	1.5	1.6
	PS−CD on G1-PPI-$(Fc)_4$ on β-CD SAM[a]	5.0	1.1	0.1
	PS−CD on G3-PPI-$(Fc)_{16}$ on β-CD SAM[a]	5.3	1.2	0.4

[a] Particle suspension dispersed in the presence of 5 mM native β-CD (molecules).

induced particle assemblies were 1.5−2.0 defects/μm^2, which is due to the strong adsorption and lack of mobility of these particles once in contact with the surface, which inhibits better ordering.

The adsorption of particles in the suspension zone was observed in both C and D of Figure 3. For easy comparison, the densities of particles adsorbed in the suspension zone were calculated over a suspension zone area of 1600 μm^2. The particle densities for PS−COOH on an NH_3^+ SAM and for PS−CD on a β-CD SAM in the absence and presence of 5 mM β-CD in the suspension zone were 0.5, 0.8, and 0.2 particles/μm^2, respectively, indicating strong interactions between the particles and the surfaces.

Figure 4 shows particle lattices formed by utilizing the specific supramolecular host−guest interactions between β-CD SAMs and ferrocenyl-functionalized dendrimers. To avoid involvement of electrostatic interaction in the assembly, PS−CD were dispersed in pH 9.0 carbonate buffer, in order to deprotonate both the dendrimers and the COOH groups on the particles' surfaces, and to increase the ionic strength in the particle suspension, such that the electrostatic interactions can be shielded. Figure 4A was obtained by assembling PS−CD particles on the larger G3-PPI-$(Fc)_{16}$ dendrimer pre-adsorbed on a β-CD SAM. The β-CD SAM became somewhat less hydrophilic upon adsorption of G3-PPI-$(Fc)_{16}$ onto the substrate (see Table 1), but still feasible for convective assembly. The particle assembly with supramolecular interaction was distinctly different from the assembly on native SiO_2 or with electrostatic interaction. Once the particle suspension was added, huge numbers of particles adsorbed instantaneously onto the dendrimer-β-CD SAM surface. This phenomenon hindered the formation of a dense particle lattice in the assembly zone. In fact, the adsorbed particles act as an obstacle for the convective flow of particles toward the assembly zone. As seen in situ by the optical microscope, the freely suspended particles had to travel in a twisted path before reaching the boundary of the assembly zone. At some point, the density of the adsorbed particles in the suspension zone was so high that the assembly was inhibited altogether and a new assembly zone started to form elsewhere. The order of the resulting particle lattice was very poor (Figure 4A). When the temperature was reduced below the dew point, most particles remained at their original position, and desorption of the particles by condensation was negligible.

The results obtained so far suggest that the particle lattices formed by additional electrostatic and/or supramolecular interaction, although very stable on the surface, fail to form perfect close packed particle lattices as a result of strong interactions between the particles and the surface. In order to form a stable and closed packed particle lattice, a few considerations have to be taken into account (i) the adsorption of particles in the suspension zone should be sufficiently low so that the influx of particles to the assembly zone will not be disturbed, and (ii) the mobility of the particles at the boundary between assembly and suspension zones has to be preserved to allow reorganization of particles into perfect hexagonal close packing.

As a result, further fine-tuning of supramolecular assembly was implemented by first using ferrocenyl dendrimer of generation 1 (G1-PPI-$(Fc)_4$). The wettability of the surface ($\theta_a = 60°$) was similar to that of G3-PPI-$(Fc)_{16}$ on a β-CD SAM. As observed during the assembly, some particles already adsorbed onto the substrate in the suspension zone. As shown in Figure 4B, the PS−CD particle lattice that formed on pre-adsorbed G1-PPI-$(Fc)_4$ on β-CD SAM was disordered. Further attempts to achieve an ordered supramolecular particle lattice were carried out by adding 5 mM native β-CD to the particle suspension. The assembly was performed on pre-adsorbed G1-PPI-$(Fc)_4$ on a

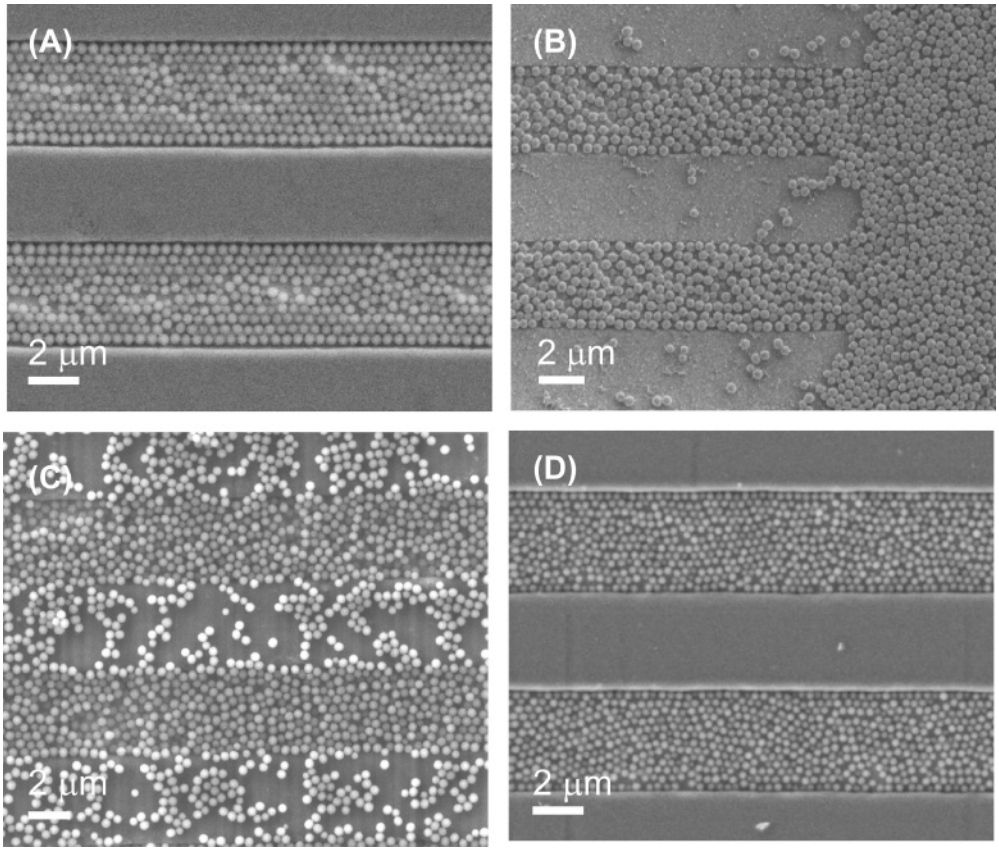

Figure 5. SEM micrographs of NIL-patterned particle lattices formed by adsorption of PS−COOH on native SiO_2 on Si (A), PS−COOH on an NH_3^+ SAM (B), and PS−CD on β-CD SAM with pre-adsorbed G1-PPI-$(Fc)_4$ in the absence (C) and presence (D) of 5 mM native β-CD.

β-CD SAM. The number of particles adsorbed on the surface in the suspension zone was reduced considerably (Table 2). As shown in Figure 4C, the packing of the particle lattice was nearly hexagonal which constitutes a drastic change from the disordered packing shown in A and B of Figure 4. The desorption of particles by condensation was negligible for the assemblies on pre-adsorbed G1-PPI-$(Fc)_4$ on β-CD SAMs, as already observed previously for G3-PPI-$(Fc)_{16}$.

As shown in Table 2, there are differences in packing order between the supramolecular particle lattices formed in the absence and presence of competitive interactions by native β-CD (molecules). The particle lattices formed in the absence of β-CD were disordered (and random), with packing densities of 4.5−4.8 particle/μm^2 and defects of 1.4 defects/μm^2. In contrast, assemblies formed in the presence of β-CD were hexagonally closed packed, with 5.0−5.3 particles/μm^2 and defect densities of 1.1−1.2 defects/μm^2 (Table 2). A reduction in adsorption of particles in the suspension zone was observed. The densities of the particles in the suspension zone were reduced from 1.6 to 0.4 and 0.4 to 0.1 particles/μm^2 for G3-PPI-$(Fc)_{16}$ and G1-PPI-$(Fc)_4$ surfaces, respectively, when 5 mM native β-CD was added to the particle suspension.

The use of G3-PPI-$(Fc)_{16}$ resulted in the highest adsorption density in the suspension zone, indicating the strong binding affinity between the particles and the surface as a result of spontaneous and strong multivalent supramolecular interactions, which makes reorganization and ordering of the particles very difficult. In comparison, G1-PPI-$(Fc)_4$, with a 50% lower Fc surface coverage than that of G3-PPI-$(Fc)_{16}$ (see Supporting Information, Figure S4) caused less particle adsorption in the suspension zone, suggesting a weaker and more dynamic host−guest interaction. Nevertheless, the interaction force of the simultaneous binding of multiple β-CD sites on a single particle to multiple Fc sites on the surface is probably still larger than the lateral capillary force between the neighboring particles, which prevents the ordering of particles.[45] With addition of native β-CD to the particle suspension, competition was initiated. Thus, after reducing the total number of interactions and inducing competition in the assembly, a nearly hexagonally close packed supramolecular particle lattice was obtained by using G1-PPI-$(Fc)_4$ with native β-CD present in the particle suspension. To our knowledge, this is the first time that supramolecular competition is shown to result in fine-tuning of interactions and ordering of materials.

Assembly of Particles on Nanoimprint Lithography Patterned Substrates. As an extension to the fabrication of nanostructures, substrates patterned by nanoimprint lithography (NIL) were employed to assemble the particles into micrometer lines. A piranha-cleaned silicon substrate with a 500-nm thick layer of PMMA was pressed against a hard stamp at high temperature to form patterned substrates with 3.5-μm wide polymer lines. The residual layer in the imprinted areas was removed by acetone. The NH_2 and β-CD SAMs were subsequently formed on the native SiO_2 according to previously described procedures.[46] Figure 5 shows the patterned particle lattices formed on nanoimprinted patterns assembled via convective assembly, with electrostatic interactions and with supramolecular host−guest interactions. For the convective assembly (Figure 5A), the particles were physically confined by the PMMA polymer barriers into the 3.5-μm wide silicon oxide areas, which resulted in the formation of highly hcp-ordered particle lines. The selective

(45) Huskens, J.; Mulder, A.; Auletta, T.; Nijhuis, C. A.; Ludden, M. J. W.; Reinhoudt, D. N. *J. Am. Chem. Soc.* **2004**, *126*, 6784.

(46) Maury, P.; Péter, M.; Crespo-Biel, O.; Ling, X. Y.; Reinhoudt, D. N.; Huskens, J. *Nanotechnology* **2007**, *18*, 044007.

particle assembly was driven by the large chemical contrast between PMMA ($\theta_a = 80°$) and silicon oxide.

In the beginning of the assembly with additional electrostatic interactions (Figure 5B), the particles bound preferentially to the NH_3^+ SAM. The particle lines were disordered and multilayered as a result of the strong electrostatic interactions of the particles with the substrate. As the wetting contrast between the NH_3^+ SAM and PMMA is relatively low, we observed that after a few seconds of assembly, the particles started to assemble on the polymer lines too. In the end, nearly all the polymer features were covered with particles. This is particularly true when the withdrawing speed was 0.5−1.0 μm/s, as also observed by Jonas et al.[47] Nevertheless, the substrate could be treated by rinsing in agitated MilliQ water to remove the particles physisorbed onto the PMMA, or in this case, PMMA and particles on PMMA can be easily "lifted off" from the substrate by rinsing with acetone.

In the case of supramolecular interaction using G1-PPI-$(Fc)_4$ and a particle suspension of high pH buffer in the absence of β-CD, a random particle lattice was formed with nonspecifically adsorbed particles everywhere (Figure 5C). The lack of specificity of the assembly is attributed to the adsorption of dendrimers onto the PMMA structures as a result of hydrophobic interactions.[48]

To fine-tune and improve the specificity of the assembly, a particle suspension with 5 mM native β-CD was used (Figure 5D). Periodic changes in hydrophilic properties and the shape of the water meniscus were clearly observed as a result of alternating dewetting and wetting effects by the PMMA and β-CD SAM areas, respectively. The nonspecific adsorption of dendrimers on PMMA was reduced as a result of competition by β-CD in solution. Hence, a well-controlled, stable, and single layer of particles was formed in the assembly process with a better degree of order than without β-CD. Potentially, this method can also yield multilayered nanostructures by repeating the adsorption of the ferrocenyl dendrimers and β-CD particle, as shown before in a layer-by-layer process for 5-nm gold particles.[13]

(47) Fustin, C.-A.; Glasser, G.; Spiess, H. W.; Jonas, U. *Langmuir* **2004**, *20*, 9114.

(48) Crespo-Biel, O.; Dordi, B.; Maury, P.; Péter, M.; Reinhoudt, D. N.; Huskens, J. *Chem. Mater.* **2006**, *18*, 2545.

Conclusions

The in situ observation of the adsorption and desorption of particles during convective assembly on native oxide surfaces with additional electrostatic interactions and with supramolecular interactions has been presented. PS−COOH particles on native SiO_2 surfaces displayed the best hcp packing among all, but these lattices can be easily desorbed by reducing the temperature below the dew point. The electrostatically induced assembly led to disordered lattices. The highly tunable supramolecular assembly, driven by multivalent host−guest interactions between PS−CD and G1-PPI-$(Fc)_4$ or G3-PPI-$(Fc)_{16}$ on β-CD SAMs resulted in a nearly hcp packing in the presence of a competing interaction by native β-CD, also providing good specificity and selectivity on NIL-patterned substrates. We envision, with the use of these specific, yet highly tunable supramolecular interactions, the buildup of more sophisticated and more complex nanostructures that cannot be achieved by physical assembly. In particular, the combination of top-down surface patterning and bottom-up material assembly that involves multivalent supramolecular interactions is anticipated to lead to well-defined 3D nanostructures.

Acknowledgment. We thank Mark Smithers for the SEM measurements, Thomas van Zanten and Dr Monique Roerdink for the construction of Voronoi diagrams. X.Y.L and J.H. thank the Council for Chemical Sciences of The Netherlands Organization for Scientific Research (NWO-CW) for financial support (Vidi Vemieuwingsimpuls Grant 700.52.423 to J.H.). We also gratefully acknowledge support from the European FP6 Integrated project NaPa (Contract No. NMP4-CT-2003-500120). The contents of this work are the sole responsibility of the authors.

Supporting Information Available: FTIR-spectra of particles, SEM image and size distribution of PS−COOH particles, zeta potentials of dispersions of PS−COOH and PS−CD, and cyclic voltammograms of G1-PPI-$(Fc)_4$ and G3-PPI-$(Fc)_{16}$ dendrimers pre-adsorbed on β-CD SAMs; video clips on the adsorption of PS−CD particles on G1-PPI-$(Fc)_4$ pre-adsorbed on a β-CD SAM in the absence and presence of 5 mM native β-CD. This material is available free of charge via the Internet at http://pubc.acs.org.

LA701671S